



Groundwater-quality probability mapping and assessment for domestic and irrigation purposes in Ghara-su Basin of Golestan Province, Iran

B. Raheli-Namin¹, S. Mortazavi^{*2}, M. Mobinifar³, M. Adeli⁴

¹ *Department of Environmental Sciences, PhD Candidate of Natural Resource and Environment, Malayer University, P.O. Box 65719-9581863, Malayer, Hamedan, Iran*

^{*2} *Assistant Professor, Department of Environmental Sciences, Faculty of Natural Resource and Environment, Malayer University, P.O. Box 65719-9581863, Malayer, Hamedan, Iran.*

**Corresponding author: Tel: +989166652008*

Fax: +98813339948 E-mail: mortazavi.s@gmail.com

³ *Department of Environment, Islamic Azad University . Kalaleh. Iran*

⁴ *Department of Geography and Urban Planning, Research Institute of Natural Crisis Engineering. Iran*

Received 23 Dec 2014, Revised 31 Oct 2015, Accepted 01 Nov 2015

** Corresponding author. E-mail address: mortazavi.s@gmail.com; Tel: (+989166652008)*

Abstract

Groundwater contamination due to agricultural activities and fast industrialization is a major concern for human communities. Applying certain monitoring techniques and a groundwater-monitoring network can reveal the critical condition of these resources. The main purposes of this investigation are to present an overview of present groundwater quality, determine the spatial distribution of some groundwater-quality indices such as Cl^- , SO_4^{2-} , EC and NO_3^{-1} , and select the best Geostatistical method for mapping groundwater quality in the Ghara-su Basin of Golestan Province, Iran. Also chemical variables were graphically interpreted using Piper, Durov and USSL diagrams to show the groundwater facies. Kriging and Cokriging methods are evaluated for mapping of groundwater quality. The analysis shows that universal Cokriging achieves better results for estimation of EC, Cl^- and NO_3^{-1} contents than other methods; for SO_4^{2-} , universal kriging is obviously more precise than other methods. Each method depends on the distribution of samples and the characteristics of the region. The groundwater-quality maps show that the highest concentrations of groundwater-quality indices are located to the North of Gorgan City, and results of graphically analysis of physico-chemical parameters indicated that Ca - Mg was the mainly water facies dominant in this area and the water type highly exhibit So_4 - Cl and most of the groundwater samples for agricultural purposes are found in C2S1 which are suitable for irrigation. A few samples in the north of the study area were unsuitable for irrigation. In general, groundwater quality decreases moving from the South to the North of the Ghara-su Basin.

Key words: Groundwater quality, Kriging, Cokriging, Probability maps, Ghara-su Basin.

1. Introduction

In recent years, the importance of groundwater as a natural resource has increased [1] One of the existing threats in many areas is the increasing amount of soluble chemicals being produced in urban and industrial activities[2] and modern agricultural practices. Groundwater resources are a crucial component of the ecosystem. This water supply is essentially a renewable resource generated from within the global water-circulation system [3]. But in many cases, groundwater is polluted by industrial wastewater and sewage [4]. People who use contaminated groundwater as drinking water may suffer from diseases in the future as a result

[5]. Many regions all over the world are entirely dependent on groundwater resources for various uses. Groundwater contaminated with various pollutants that make it unsuitable for consumption can put human and animal life as well as the overall environment at great risk.

So, specific practical actions are needed that aim to control the risk of water pollution and protect the natural quality of groundwater. GIS and Geostatistical methods can be powerful tools for producing spatial data and informing management decisions [6]. Geostatistical methods were developed to identify spatial patterns and interpolate values at unsampled locations, creating mathematical models of spatial correlation structures with a variogram [7]. Sample variograms should be estimated with the proposed function to model the spatial structure of data on water quality [8].

In recent years, many scientists have used Geostatistical methods for prediction of groundwater depth and quality, and have evaluated the accuracy of different spatial interpolation methods.

Gaus et al. [9] employed disjunctive kriging to analyse the arsenic concentration in groundwater in Bangladesh. Ahmadi and Sedghamiz [6] evaluated kriging and Cokriging methods for mapping the groundwater depth in the South-East of Fars Province, southern Iran. The results demonstrated that groundwater depths were all spatially correlated. Moreover, it was concluded that although both methods were acceptable, Cokriging gave more accurate results in mapping the groundwater depth across the study area. Nas [10] used the Ordinary Kriging (OK) method to assess the spatial distribution of groundwater quality. Dash et al. [11] applied OK and IK to analyse the spatial variability of groundwater depth and quality in Delhi; their study results indicated that the groundwater chloride levels in 62% of the study area exceeded 250 mg/L, and salinity levels in 69% of the area exceeded 2.5 dS m⁻¹. Mendes and Ribeiro [12] used Disjunctive Kriging (DJ) methods to study the spatial variability of nitrates on the Balarood Plain alluvial system of the River Tagus. Their results showed there were more areas on the western bank with higher probabilities of contamination by nitrates (nitrate concentration values above 50 mg/L) than on the eastern bank. Ghadermazi et al [13] compared Ordinary Cokriging with Ordinary Kriging and inverse distance weighting for the spatial prediction of NO₃-N in drinking water, using pH as an auxiliary variable, on the Bijar and Qorveh Plains of western Iran. Their results indicated that Cokriging achieved better results than other methods. Arslan [8] used Ordinary Kriging and Indicator Kriging for mapping spatial and temporal groundwater salinity Bafra Plain of Turkey. The results showed that, spatially, groundwater salinity showed a tendency to increase towards the North of the Bafra plain; temporally, groundwater salinity decreased from 2004 to 2010. Azareh et al. [14] developed groundwater-quality maps with the use of the Geostatistical and deterministic methods for the Shahr-e Babak Plain of Iran. Using deterministic methods, the authors found that RBF, due to having lower RMSE and MAE, is more suitable to develop a variation map of the parameters Cl, Na and TH.

According to the above-mentioned researchers' results, Geostatistical techniques can be widely and successfully used in different applications. The suitable method of interpolation depends on study area, regional factors and variable type; no single method for a specific area can be generalized to others [7].

The main purposes of this investigation were to present an overview of present groundwater quality, determine the spatial distribution of some groundwater-quality indices, such as Cl⁻, SO₄⁻², EC and NO₃⁻¹, and select the best Geostatistical method for mapping groundwater quality. In this research, Kriging and Co kriging methods are applied to assess their precision in mapping the groundwater-quality parameters in the Ghara-su Basin of Golestan Province in the North-East of Iran. This basin is a valuable ecosystem for agricultural activity due to its wet Mediterranean climate and fertile soil. Ghara-su Basin sees high annual rates of fertilizer application, which has a strong influence on groundwater quality.

2. Materials and methods

2.1. Study area

The Ghara-su Basin of Golestan Province in Iran has an area of about 1660 km². The study area is located on the northern slopes of Alborz Mountain. The catchment area has an altitude ranging from -27 m in the South-West of the Caspian Sea to 3086 m. The mean annual precipitation is about 560 mm. Gorgan City (the capital of Golestan Province) and Kordkuy are two important districts in the region. Golestan Province is one of the

most important areas of Iran for agriculture and in terms of the high density of the population; assessing groundwater quality is therefore vital. Figure 1 shows a location map and the geographical location of the observation wells. As indicated by the figure, 186 wells were analyzed and about 965 km² of the Ghara-su Basin was assessed and mapped.

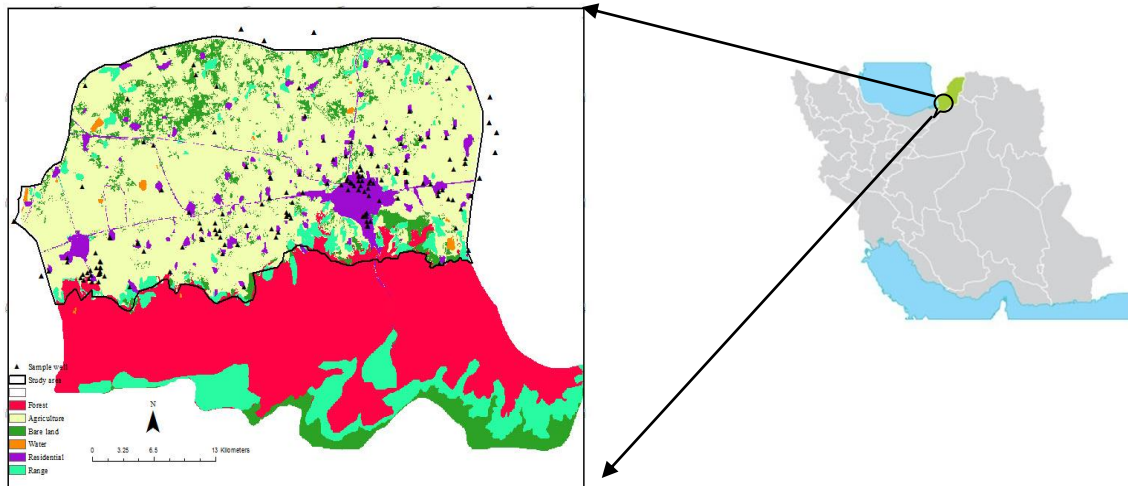


Figure 1: Location map and Land use pattern of the Ghara-Su Basin

2.2. Spatial prediction methods

Data were collected from rural Golestan water and sewer as well as water and wastewater companies. After performing a normality (Kolmogorov-Smirnov) test to analyse the normal distribution for each parameter, Kriging and Cokriging techniques were used to estimate or predict groundwater quality at unsampled locations.

2.2.1. Kriging and Cokriging methods of interpolation

The theoretical basis of Geostatistics has been described by several authors [15-17]. Semi-variograms are the main tool in Geostatistics, which express spatial autocorrelation between neighbouring observations. In fact geostatistic methods by exploitation spatial autocorrelation contained in georeferenced data are used to spatial prediction purposes and evaluate the spatial structure of a variable. Autocorrelation is evaluated using structure functions that assess the spatial structure or dependency of the variable. Semi-variance is used for descriptive analysis where the spatial structure of the data is investigated using the semi-variogram and for predictive applications where the semi-variogram is fitted to a theoretical model, parameterized, and used to predict the regionalized variable at other non-measured points. A semi-variogram shows the distance between all the pairs of available data points, as calculated using Eq. (1).

$$\gamma(h) = \frac{1}{2N} \sum_{i=1}^N [Z(x_{i+h}) - Z(x_i)]^2$$

The experimental semi-variogram can be obtained by grouping the data pairs according to their distances from the measured data points, where $\gamma_{(h)}$ is the value of the experimental variogram for a distance of h (Lag size); N is the number of data pairs at a distance of h ; x_i are the geo-referenced positions and $z_{(x_i)}$ and $z_{(x_i+h)}$ is the value of other points separated from x_i by a discrete distance h [8,13,16]. After analysis, the empirical (cross)-variogram was fitted to the theoretical variogram function to model the spatial autocorrelation curve and after comparing models; the best-fit model was chosen according to the different parameters (e.g., range, nugget and sill) and then used in the Kriging procedure.

The performance validation of the fitted models was done by cross-validation using correlation coefficients (r^2) and residual sum of squares (RSS) as criteria. The basic equation used in Ordinary Kriging (OK) is as follows:

$$Z_0 = \sum_{i=1}^n \lambda_i Z(x_i)$$

In this method the estimated mean is assumed to be constant. Simple Kriging (SK) is similar to Ordinary Kriging (OK), except that it uses the average of the entire data set while Ordinary kriging uses a local average

[10]. When a significant spatial trend is regionalized in the data values, such as a sloping surface, the assumption of the stationarity of the mean is violated and leading to a nonstationary interpolation technique the stationary condition can be temporarily imposed on the data using a simple polynomial function. Universal Kriging (UK) provides an estimator when a trend is present in the measured dataset. The trend can be modelled with the following polynomial:

$$m(x) = \sum_{p=1}^l a_p \times f_p(x)$$

Where l is the number of functions used in modelling the trend, a_p is the p th coefficient; f_p is the p th basic function that describes the trend. As shown in Figure 2, this study's variables, which included Cl^- , SO_4^{-2} , EC and NO_3^{-1} have a trend.

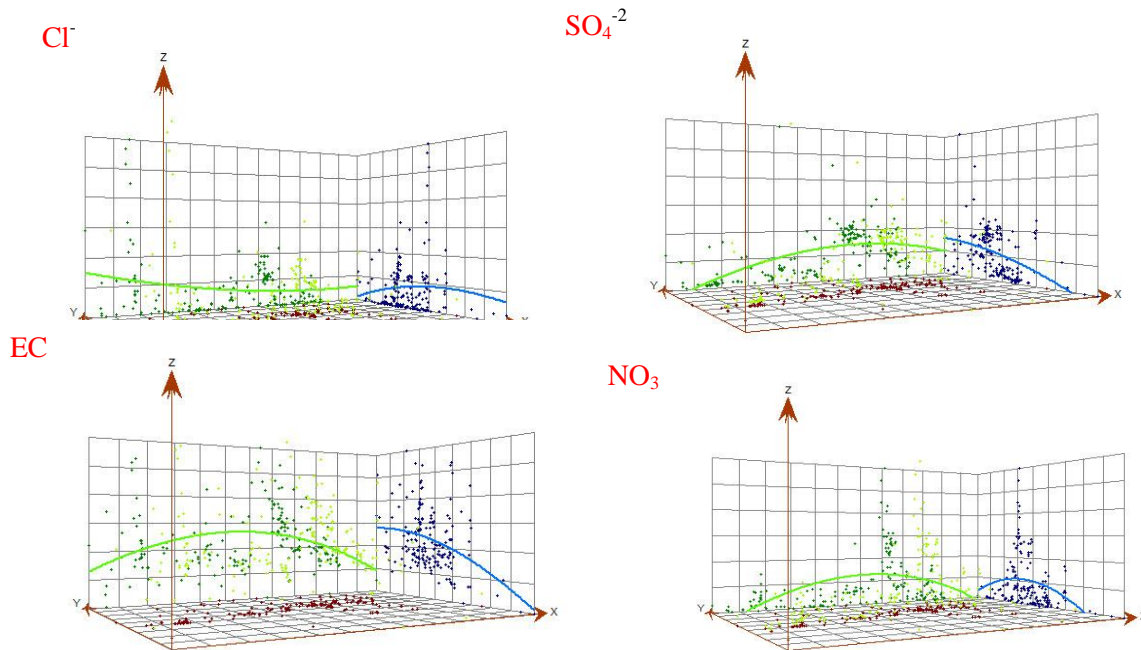


Figure 2: Tend analysis of Cl^- , SO_4^{-2} , EC and NO_3

The universal kriging predictor $Z_w^*(X_0)$ of the value of $Z(x)$ at the target point x_0 is the linear sum

$$Z_w^*(X_0) = \sum_{i=1}^n w_i Z(X_i) = W^T Z$$

With weights $w_i \in \mathbf{R}$, $i = 1, \dots, n$; corresponding to each evaluation of the random function $Z(x)$ at the sample point x_i and $W := (W_1, \dots, W_n)^T \in \mathbf{R}^n$

Whenever spatial dispersion of data is complicated and choosing the best-fit model is difficult, Disjunctive Kriging (DK) was used.

Cokriging methods are used between two or more regionalized but related variables; such methods are appropriate when data are sparse. Cokriging permits us to estimate the values of one variable with the aid of an auxiliary one[13,19]. The advantages of Cokriging include reductions in costs or sampling effort. The spatial cross-semivariance model of primary and secondary attributes is computed through the following equation:

$$\lambda_{ij}h = \frac{1}{2} E[\{z_i(x) - z_i(x+h)\}\{z_j(x) - z_j(x+h)\}]$$

where λ_{ij} is the cross-semivariance between i and j , z_i is the primary variable and the secondary variable [20].

2.2.2. Prediction performances and Comparison between the different methods

Prediction performances were assessed by Root Mean Square Error (RMSE) and General Standard Deviation (GSD) in cross-validation mode. By the cross-validation technique a table with two columns was created, consisting of real and estimated points. For the obtained estimated points, each time an observable point was temporarily omitted and the calculation of the estimated amount done for that point through nearby points. RMSE and GSD were estimated using the following formulas:

$$RMSE = \sqrt{\frac{1}{N} \sum_{i=1}^N (Z_i - Z_i^*)^2}$$

$$GSD = \frac{RMSE}{\bar{Z}_i}$$

where Z_i is the observed value at point i , Z_i^* is the predicted value at point i , N is the number of samples and \bar{Z}_i is the average of observable amounts. The smallest RMSE and GSD values indicate the most accurate predictions[21,22].

2.3. The assessment of groundwater quality

Some groundwater-quality indices such as Cl^- , SO_4^{-2} , EC and NO_3^{-1} were used for mapping and assessing spatial distribution of them based on Geostatistical method. Also, Chemical variables were graphically interpreted using Piper, Durov and USSL diagrams to show the groundwater facies for Ghara-su Basin of Golestan Province. To understand general chemical nature of groundwater, Piper trainer diagram (Piper, 1944) is used. Durov, (1948) introduced another diagram which an alternative to the Piper diagram and display some possible geochemical processes by providing more information on the hydro-chemical facies. For determination of suitability for irrigation use the US Salinity Laboratory Staff (USSL 1954) diagram by plotting the value of sodium absorption ratio (SAR) and electrical conductivity (EC). The SAR is computed using the formula [23, 24]

$$SAR = \frac{Na}{\sqrt{\frac{Ca + Mg}{2}}}$$

3. Results and discussion

3.1. Descriptive statistics

Table 1 provides a summary of groundwater-quality statistics such as mean, standard deviation, minimum, maximum, coefficient of variations of skewness, and kurtosis and were used to mapping . Kriging methods work best if data are normally distributed; this study’s variables, which included Cl^- , SO_4^{-2} , EC and NO_3^{-1} , exhibited a non-normal distribution of measured values, and therefore a logarithmic method was used for data normalization.

Table 1: Summary of groundwater quality statistics (Cl^- , SO_4^{-2} , EC and NO_3^{-1} were used for mapping)

GWQI	Min	Max	Mean	Std	Kurtosis	Skewness
Cl^-	1	411.200	55.8872	64.7815	11.36	2.88
Cl^{-*}	0	6.02	3.024	1.572	-1.15	-.35
SO_4^{-2}	10	370	74.6449	53.0550	4.74	1.40
SO_4^{-2*}	2.3	5.91	4.035	.792	-1.11	-.27
EC	300	1448	795.333	236.464	.12	.61
EC*	5.70	7.28	6.635	.302	.38	-.27
NO_3^{-1}	1	80	12.081	15.507	3.22	1.83
NO_3^{-1*}	0	4.38	1.698	1.29	-1.20	.29

Figure 3 shows the variables histogram before and after normalization. Also Table 2 provides the Statistical summary of Physico-chemical Parameters which were used to graphically analysis.

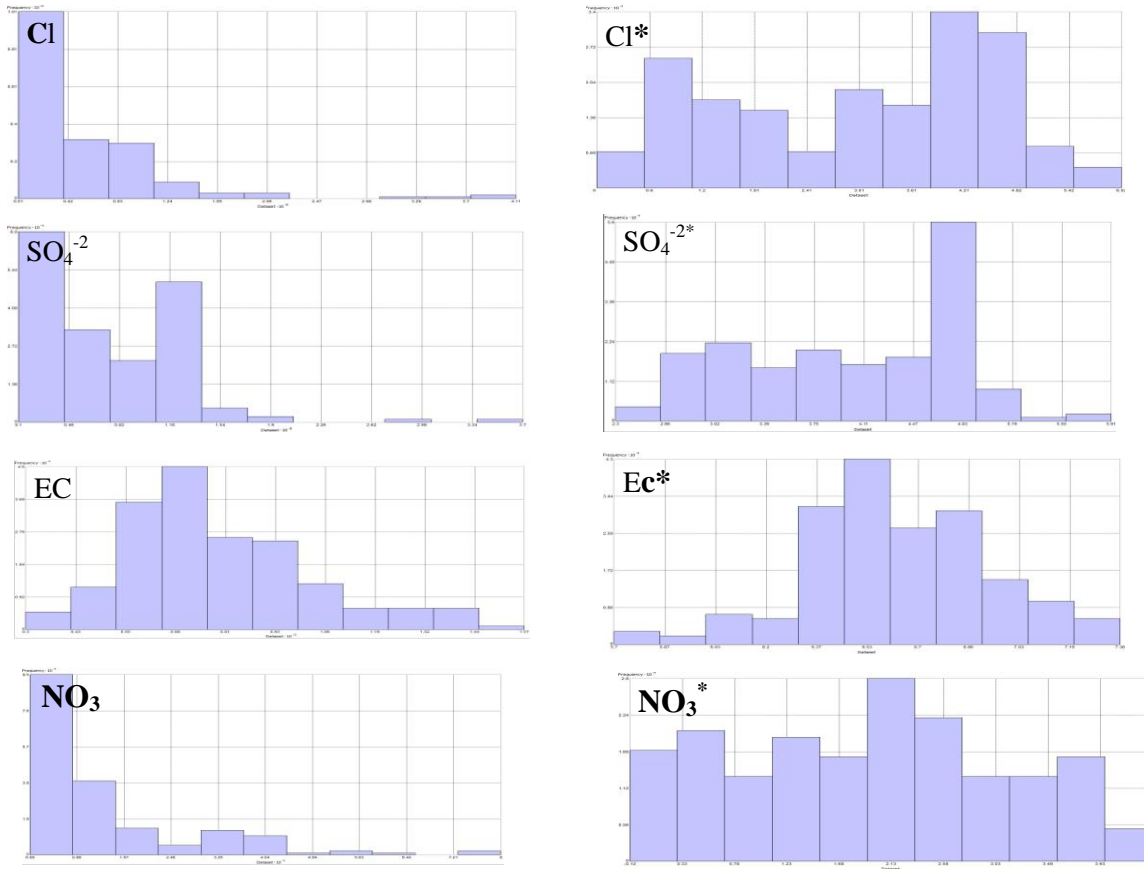


Figure 3: Data histogram of Cl^- , SO_4^{2-} , EC and NO_3^- before and after normalization of data distribution. a) Before normalization of data distribution. b) After normalization of data distribution.

Table 2: Statistical summary of Physico-chemical Parameters

	Mg	TDS	Na	Ph	K	Ca
Min	4.8	191.5	1.15	6.87	0.2	28.8
Max	53.76	988.5	200.1	8.1	20.28	153.6
Mean	26.894	472.56	40.402	7.506	2.23	80.012
STD	9.494	141.113	32.9	0.232	1.981	23.143

3.2. Semi-variogram and cross-semivariance models

The software GS^+ was used for the Geostatistical analysis. Table 3 shows the selected variogram models, which fitted best to the experimental or sample values.

These included Spherical (EC) and Gaussian (SO_4^{2-} , Cl^- and NO_3^-) quadratic models. These semi-variograms are shown in Figure 4. The spatial dependence of groundwater quality was assessed by the ratio (%) of nugget to sill, a ratio of <25% indicating a strong spatial dependence, a ratio of 25–75% indicating moderate spatial dependence, and a ratio of >75% indicating a weak spatial dependence. The results for the nugget-to-sill ratios indicated a moderate spatial structure of groundwater quality for Cl^- , NO_3^- and EC, and a weak spatial structure for SO_4^{2-} (Table 3).

Table 3: Best-fitted variogram models of ground water quality and their parameters

Groundwater quality	Model	(Co) Nugget	(CO+C) Sill	Range effect (m)	(CO/CO+C) %	R ² %	RSS
Cl ⁻	Gaussian	2.4130	4.8270	41100	51	62	0.045
SO ₄ ⁻²	Gaussian	0.161	2.02	33950	92	96	0.033
EC	Spherical	0.0295	0.084	3500	64	54	2.250e-03
NO ₃ ⁻¹	Spherical	0.282	1.579	17280	62	94	0.08

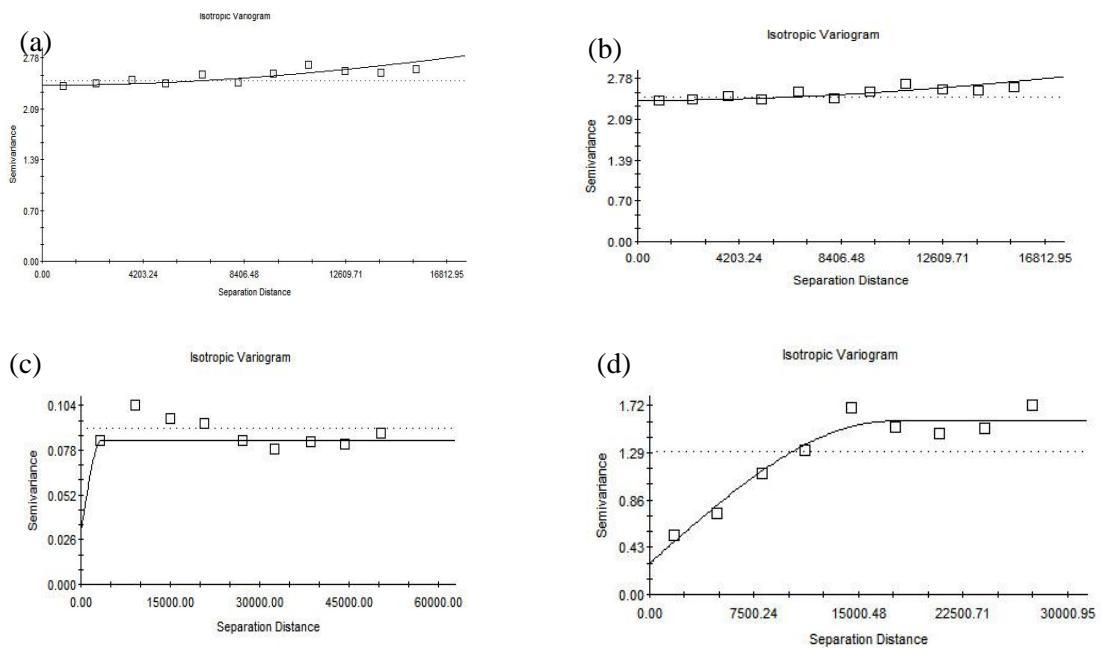


Figure 4: semi-variograms related to Groundwater quality (a) Cl⁻, (b) SO₄⁻², (c) EC and (d) NO₃

Cokriging methods are used for two or more related variables. Table 4 shows the correlation between variables. In order to apply Cokriging methods a cross-semivariance analysis must be performed prior to Cokriging. The auxiliary variables were used to develop the cross-variograms [7,20], presented in Figure 5.

Table 4: Best-fitted Cross variogram models of ground water quality and their parameters

Groundwater quality	The auxiliary variable/ Correlation index%	Model	(Co) Nugget	(CO+C) Sill	Range effect (m)	(CO/CO+C) %	R ² %	RSS
Cl ⁻	EC/ 659**	Exponential	0.1841	0.4582	34640	598	61	5.980 E-03
SO ₄ ⁻²	Ca ⁺² / 634**	Gaussian	0.0001	0.20020	71020	75	72	0.01
EC	TDS/ 955**	Spherical	0.077	0.155	21100	50	56	5.689 E-03
NO ₃ ⁻¹	Ca ⁺² / 668**	Spherical	0.001	0.323	29570	0.72	90	9.057 E-03

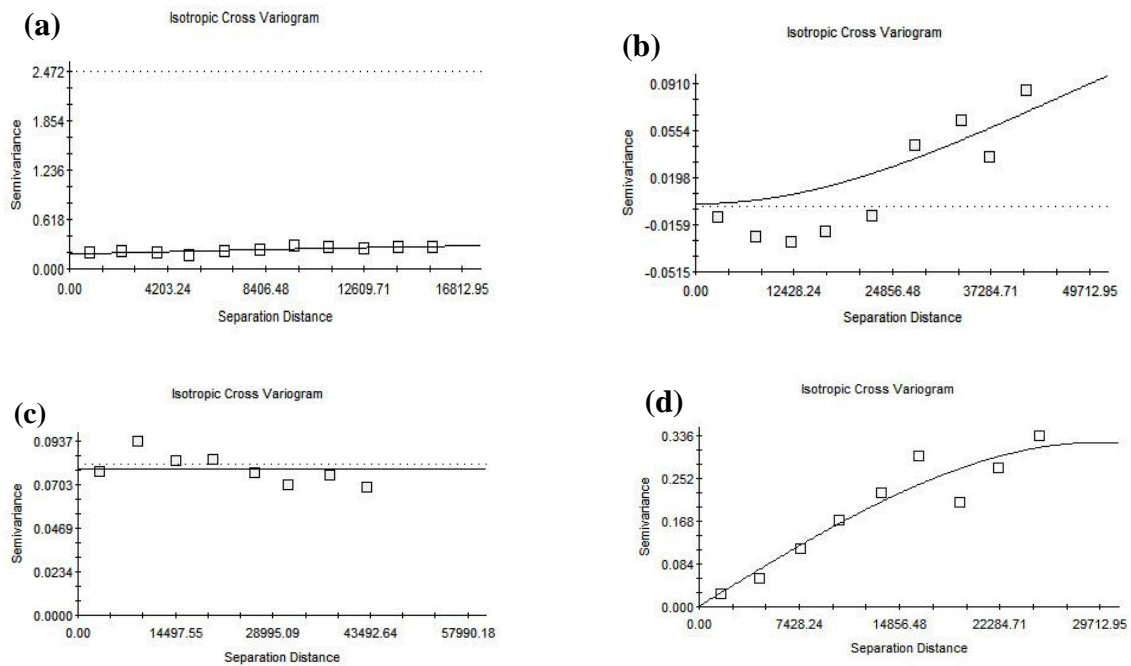


Figure 5: Cross variogram related to Groundwater quality (a) Cl⁻, (b) SO₄⁻², (c) EC and (d) NO₃

The results indicate that spherical (EC), Gaussian (SO₄⁻²) and exponential (Cl⁻ and NO₃⁻¹) quadratics are the best-fit cross-variogram models.

3.3. Selecting the best interpolation method

For selection of the most suitable method among Kriging and cokriging series, RMSE and GSD were used (Table 5).

Table 5: Selecting the best interpolation method according to RMSE and GSD parameters

GWQI		Kriging				Co-kriging			
		OK	SK	UK	DK	OCK	SCK	UCK	DCK
Cl ⁻	RMSE	163.505	177.82	159.101	177.824	61.747	64.520	60.269	64.52
	GSD	3.198	3.4783	3.1121	3.4783	1.207	1.2620	1.1789	1.262
SO ₄ ⁻²	RMSE	40.456	40.660	39.4864	40.6600	40.314	40.315	40.316	40.3153
	GSD	0.5419	0.5447	0.52899	0.54470	0.54008	0.5400	0.5401	0.54009
EC	RMSE	202.29	203.05	233.777	203.059	200.53	201.33	199.99	200.091
	GSD	0.2556	0.256	0.2954	0.2566	0.2533	0.2544	0.2527	0.2528
NO ₃	RMSE	8.2765	8.385	8.1468	8.3895	7.8369	7.8361	7.8126	7.8524
	GSD	0.638	0.647	0.6287	0.6474	0.6048	0.6047	0.6029	0.6060

The results show that Cokriging methods gave considerably more accuracy than Kriging methods for EC, Cl⁻ and NO₃⁻¹. Analysis showed that for estimation of EC, Cl⁻ and NO₃⁻¹ content Universal Cokriging (UCK) achieved better results than other methods, and for SO₄⁻² Universal Kriging (UK) was obviously more precise than other methods. If the primary variable is difficult or expensive to measure, predicting the values of one variable with the aid of an auxiliary one can greatly improve interpolation estimates without having to more intensely sample the primary variable. Finally, maps of groundwater quality were prepared by the selected best methods for interpolation in a GIS environment [7,14,20].

3.4. The groundwater-quality map

The groundwater-quality maps generated by the selected (cross) semivariograms models for each parameter are presented in Figure 6. Table 6 shows the differences in groundwater-quality values within the study area.

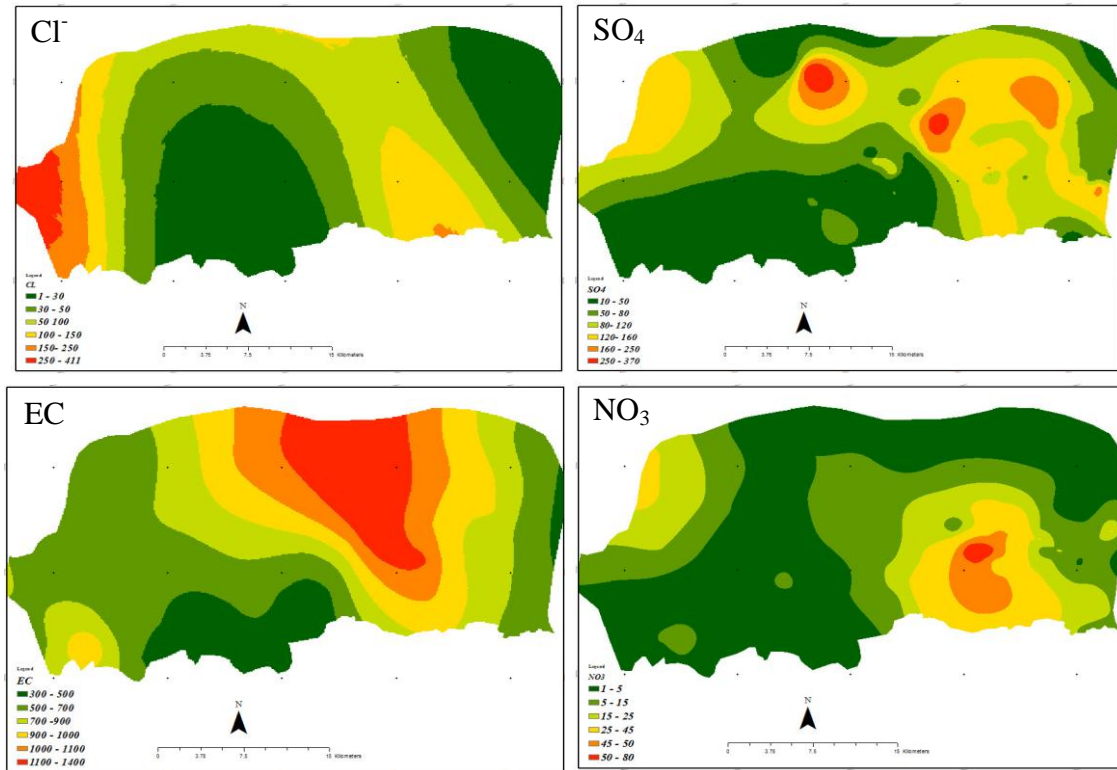


Figure 6: Spatial distribution of a Chloride, b Sulfate, c Electrical conductivity, and d Nitrate concentrations

Table 6: Selecting Differences in groundwater quality values within the study area

Groundwater quality(mg/li)	1-5 Area (km2) / %	5-15 Area (km2) / %	15-25 Area (km2) / %	25-45 Area (km2) / %	45-50 Area (km2) / %	>50 Area (km2) / %	WHO (mg/l)
NO ₃	415.81 / 43	302.79 / 31.37	134.84 / 14	79.43 / 8.22	28.54 / 2.95	3.79 / 0.39	50
Groundwater quality(mg/li)	1-50 Area (km2) / %	50-100 Area (km2) / %	100-150 Area (km2) / %	150-200 Area (km2) / %	200-250 Area (km2) / %	>250 Area (km2) / %	WHO (mg/l)
Cl ⁻	312.33 / 32.3	209 / 21.67	280 / 29	106.77 / 11	40.46 / 4.2	16 / 1.65	250
SO ₄	268.42 / 27.83	218.91 / 22.70	232.56 / 24.1	192.58 / 19.96	42.86 / 4.44	9.3 / 0.96	250
Groundwater quality (microS/cm)	1-500 Area (km2) / %	500-650 Area (km2) / %	650-800 Area (km2) / %	800-950 Area (km2) / %	950-1300 Area (km2) / %	>1300 Area (km2) / %	WHO
EC	95 / 9.8	321.6 / 33.34	185.27 / 19.2	142.32 / 14.75	110.15 / 11.41	110.22 / 11.42	

Also Standard deviation map for all produced maps and cross validation diagram between computed and estimated values were presented in figure 7 and 8.

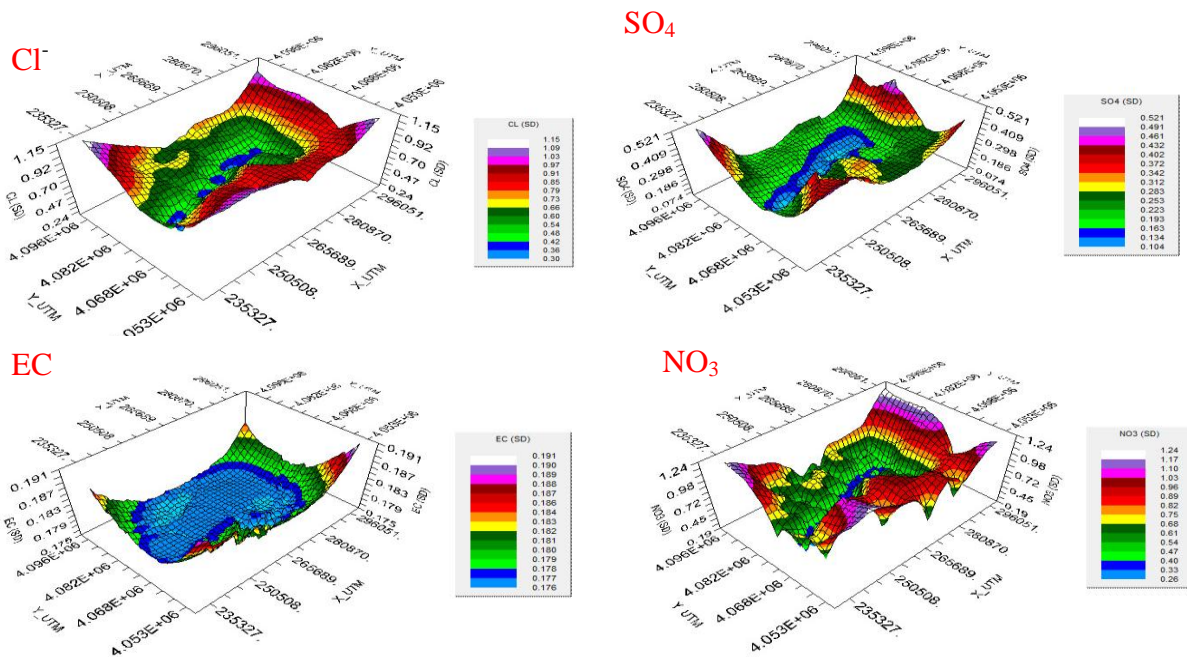


Figure 7: Standard deviation map a Chloride, b Sulfate, c Electrical conductivity, and d Nitrate

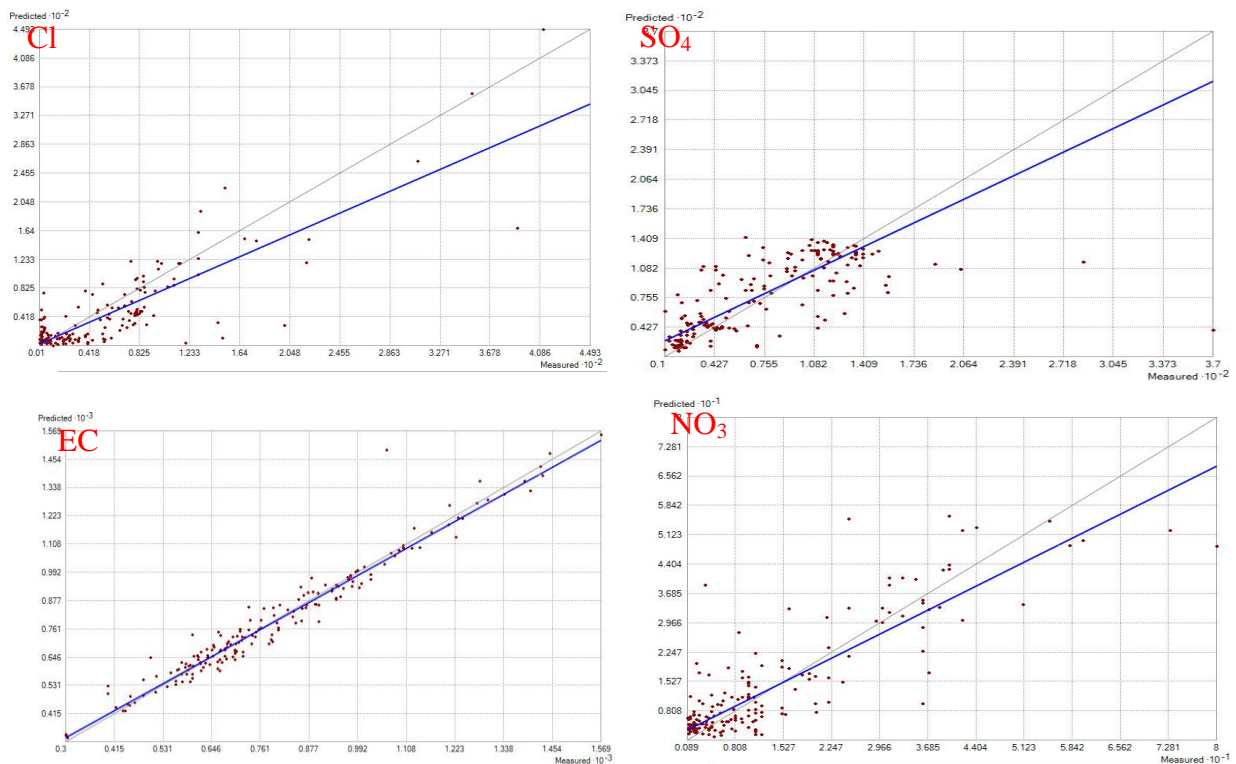


Figure 8: cross validation diagram between computed and estimated values a Chloride, b Sulfate, c Electrical conductivity, and d Nitrate

Chloride

Chloride is found in groundwater due to weathering, leaching of soil and rocks, and human activities. As indicated by Figure 6(a), high concentration of chloride gives an undesirable taste to water. The highest concentration of chloride was found in the North-West of the study area, near Caspian Sea. Saltwater intrusion

and sea spray in coastal areas are sources of chloride in groundwater [25]. The maximum contaminant level (MCL) for chloride in drinking water is given as 250 mg/l by the World Health Organization (WHO)[26]. As shown in Table 6, only in 1.65% of the study area (16 km²) did chloride concentration exceed 250 mg/li. The dispersion map shows that the concentration of chloride increased around Gorgan City due to wastewater and sewage contamination.

Sulphate

Sulphates occur naturally in numerous soil and rock formations that contain sulphate minerals. Minerals that contain sulphate include magnesium sulphate (Epsom salt), sodium sulphate (Glauber's salt), and calcium sulphate (gypsum)[27]. Sulphates can discharge into water from smelters and from kraft pulp and paper mills, textile mills and tanneries[26]. As indicated by the dispersion map, the highest concentration of sulphates was around 370 mg/l in Gorgan City. Due to the use of chemical fertilizers (mainly CuSO₄) in rice fields, sulphate concentration increases, spatially, where cultivated lands have a high density. But in 0.96% of Ghara-su Basin sulphate concentration exceeds the MCL level (WHO, 2004), as shown in Table 6.

Electrical conductivity

Conductivity is linked directly to the total dissolved solids (TDS). Total dissolved solids (TDS) comprise inorganic salts and small amounts of organic matter dissolved in water [28]. Salinity in the region increased with decreases in height, which could be because of leaching of salts through irrigation and precipitation. As shown in Figure 6c, the EC value increases from South to North, with the upper ranges greater than 1000 µS/cm; in about 11.42% of the study area (110.22 km²), EC concentration exceeds 1300 µS/cm (Table 6).

Nitrate

Urbanization and population growth in the past decade, plus changes in farming systems leading to high levels of chemical fertilizer application on vegetable fields, have had large impacts on water quality, and especially on nitrate dispersion [29]. The MCL of nitrate is given as 50 mg/l for drinking water by the WHO. As indicated in Table 6, nitrate concentrations in 3.79 km² of the study area were greater than 50 mg/l, and in 28.54 km² of the study area greater than 46 mg/l. A high average nitrate concentration (80 mg/l) was located around Gorgan City. Urbanization significantly increases the surface water-flow to rivers, and water's travel time to groundwater becomes shorter [30,31].

3.5. Graphically Representation of Physico-chemical Parameters

Piper and Durov diagrams

As shown in figure 9, Piper trainer diagram is used to characterize and analysis different water types and as mentioned earlier Durov *diagram is an* alternative to the Piper diagram.

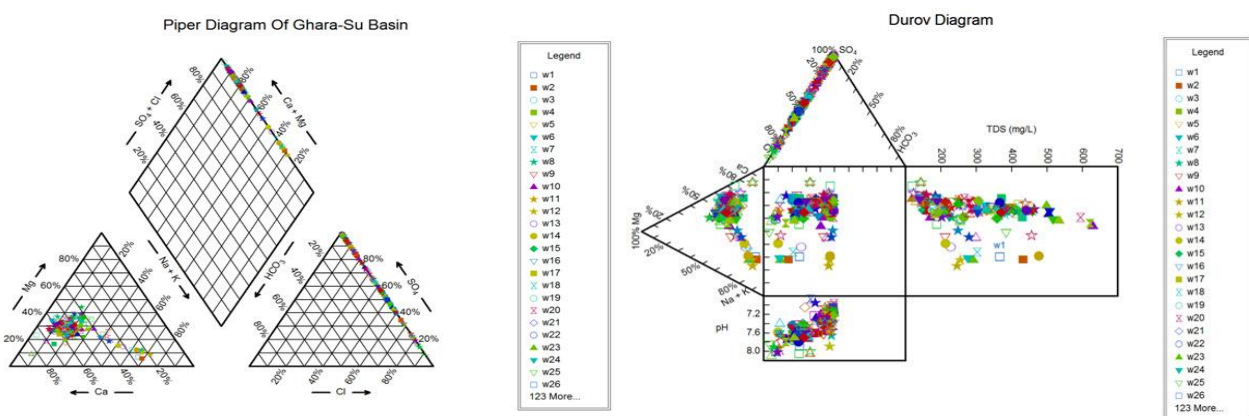


Figure 9: Ground water samples plotted on Piper and Durov diagrams

Ca - Mg was the mainly water facies dominant in this area and the water type highly exhibit So4- Cl. soluble substances of groundwater is very high. The pH part of the diagram shows that groundwater in study area is towards alkaline which is preferred for drinking

USSL Diagram

.S. salinity laboratory (USSL) has designed help to interpret the combined effect of salinity and sodium hazards. According to USSL diagram (Figure 10) most of the groundwater samples (148 well) for agricultural purposes fall under C2S1 which are suitable for irrigation. Based on this classification, about 17 (9.13%) groundwater samples represented the C3S1 (high salinity with low sodium) type and 8 (4.3%) samples are found in C3S2 class with high salinity and medium alkalinity hazards respectively and special management plane for salinity control is necessary. About 2.2 and 3.2 percent of samples in the north of the study area were grouped under C3S3 and C3S4 (which is unsuitable for irrigation). Analytical results of the USSL chart summarized in Table 7

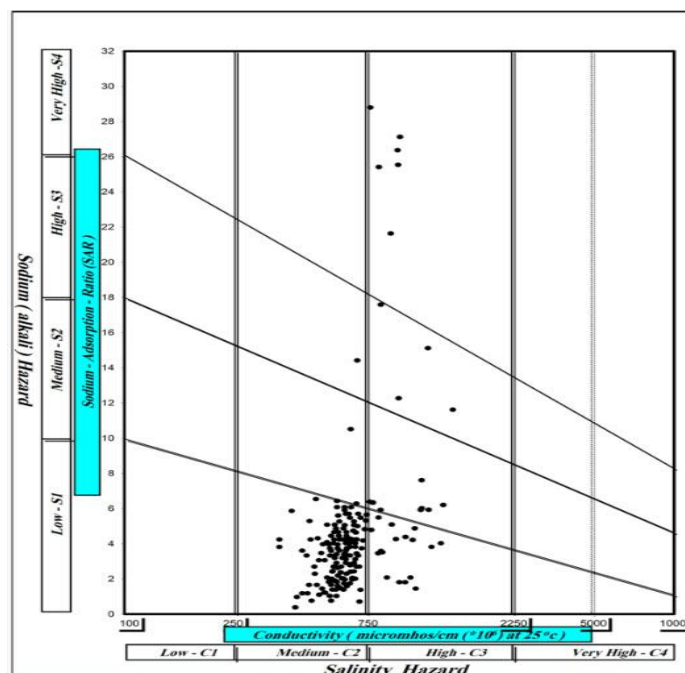


Figure 10: Suitability of groundwater for irrigation in US Salinity Laboratory Staff (USSL 1954) diagram

Table7: Ground water classification for irrigation according to USSL diagram

Water class US salinity diagram	Number of sample	percentage
C2S1 (medium EC low SAR)	148	79.6
C2S2 (medium EC medium SAR)	2	1.1
C2S3 (medium EC high SAR)	1	0.53
C3S1 (high EC low SAR)	17	9.13
C3S2 (high EC medium SAR)	8	4.3
C3S3 (high EC high SAR)	4	2.2
C3S4 (high EC very high SAR)	6	3.2

Conclusion

In this study, Geostatistical methods (Kriging and Cokriging) were applied to assess their precision in mapping groundwater-quality parameters such as Cl⁻, SO₄⁻², EC and NO₃ and Chemical variables were graphically interpreted using Piper, Durov and USSL diagrams to show the groundwater facies for Ghara-su Basin of Golestan Province in the North-East of Iran. The results of Geostatistical methods indicated a moderate spatial structure to

groundwater quality for all data. Moreover, it was concluded that for estimation of EC, Cl⁻ and NO₃ content universal Cokriging gave more accurate results in the mapping of these parameters, and for SO₄²⁻ Universal Kriging. Our study emphasizes that each method depends on the distribution of the sample and the characteristics of the region. The groundwater-quality maps show that the highest concentrations of the groundwater-quality parameters are located North of Gorgan City. Also results of *Graphically analysis of Physico-chemical Parameters* showed that Ca - Mg was the mainly water facies dominant in this area and the water type highly exhibit So4- Cl and most of the groundwater samples for agricultural purposes are found in C2S1 which are suitable for irrigation. A few samples in the north of the study area were unsuitable for irrigation. In general, the groundwater quality decreases moving from South to North in the Ghara-su Basin.

References

1. Gyanaanath G., Islam S.R., Shewdikar S.V., *Indian J. Env. Prot.* 21 (2001) 289.
2. Lee S.M., Min K.D., Woo N.C., Kim Y.J., Ahn C.H., *Environ. Geol.* 44 (2003) 210.
3. Hwang S.I., Lee S.H., Lee D.S., *J. Soil. Groundw. Environ.* 4 (1997) 122.
4. Almasri M.N., Kaluarachch J., *Environ. Model. Softw.* 20 (2005) 851.
5. Ahn H.I., Chon H.T., *Environ. Geochem. Health.* 21 (1999) 273.
6. Ahmadi S.H., Sedghamiz A., *Environ. Monit. Assess.* 138 (2008) 357.
7. Taghizadeh-Mehrjardi R., *J. Mater. Environ. Sci.* 5 (2014) 530.
8. Arslan H., *Agric. Water. Manage.* 113 (2012) 57.
9. Gaus I., Kinniburgh D. G., Talbot J. C., Webster R., *Environ. Geol.* 44 (2003) 939.
10. Nas B., *Pol. J. Environ. Stud.* 18 (2009) 1073.
11. Dash J.P., Sarangi A., Singh D.K., *Environ. Manage.* 45 (2010) 640.
12. Mendes M.P., Ribeiro L., *Sci. Total. Environ.* 408 (2010) 1021.
13. Ghadermazi J., Sayyad Gh., Mohammadi J., Moezzi A., Ahmadi F., Schuli, R., *Procedia. Environ. Sci.* 3 (2011) 130.
14. Azareh A., Mohseni Saravi M., Keshavarzi A., *IJARR.* 3 (2013) 590.
15. Isaaks E.H., Srivastava R.M., *An Introduction to Applied Geostatistics, Oxford University Press, Oxford.* 1989.
16. Oliver M.A., Webster R., *Catena.* 113 (2014) 56.
17. Xie Y., Chen T.B., Lei M., Yang J., Guo Q.J., Song B., Zhou X. Y., *Chemosphere.* 82 (2011) 468.
18. Castrignanó A., Barbeti R., Sollitto D., *Catena.* 77 (2009) 28.
19. Lichtenstern A., *TUM.* 1 (2013)105.
20. Georgakarakos S., Kitsiou D., *Hydrobiologia.* 612 (2008) 155.
21. Tutmez B., Hatipoglu Z., *Ecol. Inform.* 5 (2010) 311.
22. Ahmadian M., Chavoshian M., *Ann. Biol. Res.* 3 (2012) 5304.
23. Shimaa M., Ghoraba ., Khan A.D., *IJRRAS.* 17 (2013) 199.
24. Sivasankar V., Omine K., Msagati T. A. M., Senthil k. M., Chandramohan, A. *Arab J Geosci.* 7 (2013) 3117.
25. Deshmukh, k.k., *Int. Res. J. Environmen Sci.* 2 (2013) 66.
26. W.H.O. Organization, Guidelines for drinking water quality, *WHO, Geneva,* 2004.
27. Yongjun J., Daoxian Y., Shiyou X., Linli L., Gui Z., Raosheng H., *J. Geogr. Sci.* 16 (2006) 405.
28. Nas B., Berktaay A., *Environ. Monit. Assess.* 160 (2010) 215.
29. Babiker I.S., Mohamed A. A., Terao H., Kato k., Ohta k., *Environ. Int.* 29 (2004) 1009.
30. Inoue Y., Dabrowska-Zierinska K., Qi J., *Int. J. Environ. Stud.* 69 (2012) 443.
31. Jinno K., Tsutsumi A., Alkaeed O., Saita S., Berndtsson, R., *Hydrolog. Sci. J.* 54 (2009) 300.